Chaos control of parametric driven Duffing oscillators

Leisheng Jin, Jie Mei, and Lijie Li

Citation: Applied Physics Letters **104**, 134101 (2014); doi: 10.1063/1.4870295
View online: http://dx.doi.org/10.1063/1.4870295
View Table of Contents: http://scitation.aip.org/content/aip/journal/apl/104/13?ver=pdfcov
Published by the AIP Publishing

Chaos control of parametric driven Duffing oscillators

Leisheng Jin, Jie Mei, and Lijie Li[a)]
College of Engineering, Swansea University, Swansea SA2 8PP, United Kingdom

(Received 22 August 2013; accepted 20 March 2014; published online 1 April 2014)

Duffing resonators are typical dynamic systems, which can exhibit chaotic oscillations, subject to certain driving conditions. Chaotic oscillations of resonating systems with negative and positive spring constants are identified to investigate in this paper. Parametric driver imposed on these two systems affects nonlinear behaviours, which has been theoretically analyzed with regard to variation of driving parameters (frequency, amplitude). Systematic calculations have been performed for these two systems driven by parametric pumps to unveil the controllability of chaos.
 [http://dx.doi.org/10.1063/1.4870295]

The research of nonlinear dynamics of the resonators has attracted many attentions due to their recent implementation in micrometre and nanometre scales.[1,2] The application of such micro and nanoresonators has recently been expanded to high sensitivity sensors,[3,4] and nonlinear energy harvesting devices.[5] Duffing resonator is a classical dynamic system, known for its additional cubic spring constant, which is the main cause of the nonlinearity. Duffing oscillators can be excited to chaotic vibrations at certain driving conditions. There have been two cases where Duffing system could vibrate chaotically. A ferromagnetic cantilever enclosed in a frame with two permanent magnets magnetizing the tip of the cantilever vibrates under an external excitation applied to the frame (schematically shown in Figure 1(a)). This oscillation system has been experimentally investigated and has exhibited chaotic vibrations.[6] Magnetic forces applied on the cantilever cause the dynamic system exhibiting negative linear spring constant. The other type of Duffing resonator that could have chaotic vibrations is the clamped-clamped beam with a parametric pump.[7] The periodic behaviour of this type of oscillators has been experimentally demonstrated for miniaturized devices.[8] In terms of polarity of the spring constant, we categorized Duffing oscillators into two types with negative and positive linear spring constants, respectively. Parametric driven Duffing oscillators with positive linear spring constant have been extensively studied in the context of MEMS (Microelectromechanical Systems).[9] MEMS oscillators utilising parametrically excited non-interdigitated combdrive actuators have been designed and characterized to demonstrate the tuning of oscillator stiffness.[10] The presence of chaos was also discovered in this type of MEMS oscillators.[11] Experimental study of dynamic bifurcation, especially at edge of instability in a MEMS resonator has been presented in Ref. 12. Bifurcation of MEMS Duffing resonators were investigated using a bi-state controller.[13] This bi-state control of parametric resonance was further detailed in Ref. 14. Spring softening and hardening phenomena of an electrostatically actuated MEMS combdrive resonator has been analyzed theoretically in Ref. 15. The next paradigm shift for research in nonlinear vibrations of these two Duffing systems is to unveil whether the nonlinearity can be precisely controlled. In this work, we added a parametric pump to the system with negative spring constant to investigate controllability of chaos and adjusted driving conditions to the parametric driven Duffing system with positive spring constant to investigate chaos control.

For the negative spring constant system shown in Figure 1(a), there is a non-dimensionalized expression to describe its dynamic behaviour.[6] For the purpose of investigating chaos controllability, herein we introduced a parametric driver by adding a variable term $-A\cos(\omega_p t)$ to the linear spring constant. The new non-dimensionalized equation for the motion along z-axis of this system becomes

$$\ddot{z} + \delta\dot{z} + (\beta - A\cos\omega_p t)z + \alpha z^3 = \gamma\cos\omega t, \tag{1}$$

where δ is the linear damping rate, β and α are the linear and cubic spring constants, respectively. γ is the amplitude of the external harmonic excitation. A is the amplitude of the parametric pump. ω and ω_p are the frequencies of the external excitation and the pump, respectively. t is the time series. Simulation was performed for the un-pumped scenario ($A = 0$) using the same parameters in Ref. 16 to validate the method. The simulated Poincare diagram, shown in Figure 1(c), closely matches.[16] To predict, whether the Eq. (1) has chaotic solutions, Melnikov's method is applied.[17,18] In order to conduct Melnikov analysis, Eq. (1) is rewritten as

$$\begin{aligned} \dot{x} &= y \\ \dot{y} &= -\beta x - \alpha x^3 + \varepsilon(-\delta' y + \gamma'\cos(\omega t) + A'\cos(\omega_p t)x), \end{aligned} \tag{2}$$

where $x = z$, $y = \dot{z}$, $\varepsilon\delta' = \delta$, $\varepsilon\gamma' = \gamma$, $\varepsilon A' = A$, ε is a small parameter, hence the unperturbed form of the Eq. (2) is

$$\begin{aligned} \dot{x} &= y \\ \dot{y} &= -\beta x - \alpha x^3. \end{aligned} \tag{3}$$

Equation (3) is a Hamiltonian system. Its Hamiltonian can be expressed as

$$H = \frac{1}{2}y^2 + \frac{1}{2}\beta x^2 + \frac{1}{4}\alpha x^4. \tag{4}$$

The Hamiltonian is conserved. One can derive easily that Eq. (3) has two homoclinic orbits $\Gamma_{\pm}$, which are given by

[a)]Email: L.Li@swansea.ac.uk

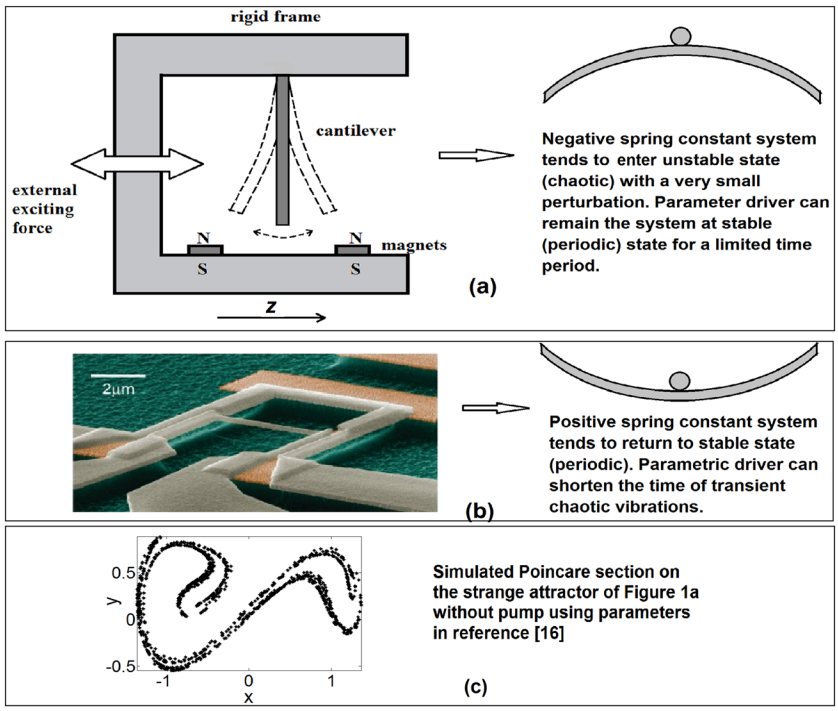

FIG. 1. (a) Schematic picture of a Duffing oscillating system with negative spring constant. Figure 1(b) Scanning electron micrograph on the left shows a device made by Roukes group. (Reprinted with permission from R. B. Karabalin, X. L. Feng, and M. L. Roukes, Nano Lett. **9**, 3116 (2009). Copyright 2009 American Chemical Society.[7]) In this type of systems, from theoretical analysis presented in this paper, chaos can be remained for a limited time period. Figure 1(c) simulated Poincare section of the non-parametric strange attractor for verifying the method.

$$\Gamma_{\pm} : (x_0(t), y_0(t)) = \left(\pm\sqrt{2}Sech(t), \mp\sqrt{2}Sech(t)\cdot\tanh(t)\right). \tag{5}$$

In Eq. (5), $x_0(t)$ and $y_0(t)$ correspond the coordination of a specific point on the orbit. Moreover, $x_0(t)$ and $y_0(t)$ will be used in solving the Melnikov function. The Melnikov function $M(t_0)$ of Eq. (2) is then obtained as

$$M(t_0) = \int_{-\infty}^{\infty} [y_0(-\delta y_0 + \gamma\cos\omega(t+t_0) + A\cos\omega_p(t+t_0)\cdot x_0)]dt, \tag{6}$$

t_0 is the time of flight from a point $(x_0(t), y_0(t))$ to the point $(x_0(0), y_0(0))$ on the homoclinic connection. Substituting (5) into (6), Eq. (6) is then re-organized into three integrals summed together, $M(t_0) = M_1 + M_2 + M_3$

$$M(t_0) = -\frac{4}{3}\delta \pm \sqrt{2}\gamma\pi\omega\, Sech\left(\frac{\pi\omega}{2}\right)\sin(\omega t_0) + A\pi{\omega_p}^2 Csch\left(\frac{\pi\omega_p}{2}\right)\sin(\omega_p t_0). \tag{7}$$

According to the Melnikov method, the first variation of distance function between stable and unstable manifolds of homoclinic orbits is proportional to Melnikov function. When chaotic motion arises in the system, there exist simple zeros in the Melnikov function (7), which implies stable and unstable manifolds intersect transversely with each other. Parameters in Eq. (7) will be carefully chosen in order to have real root t_0, which indicates that the system can possibly be at the chaotic state. It should be noted that the Melnikov method is a necessary condition. In this paper, in order to conduct a quantitative study on the parametric effect to the Duffing system, we choose $\delta = 0.2$, $\beta = -1$, $\alpha = 1$, $\gamma = 0.3$, $A = 0.2$, $\omega = 1$; and $\omega_p \in [0.8, 10]$ as a varying parameter. The system remains in the chaotic state when $\omega_p = 0$.[17] The varying range of the ω_p is selected according to the Melnikov function described above. As the pump frequency ω_p increases from 0.8ω to 10ω, solving Eq. (2) will find out the impact to the system nonlinearity due to the pump frequency ω_p. To unveil this impact quantitatively, Maximum Lyapunov exponent (MLE) of Eq. (1) will be calculated. MLEs are used to indicate the separation rate of two nearby trajectories in a chaotic system. MLEs of system described by Eq. (1) have been calculated numerically as pump frequency ω_p varying from 0.8ω to 10ω, and results are shown in Figure 2(a). It is seen from the results that the MLE is only negative as ω_p is ω, 1.5ω, 2ω, 3ω, respectively, meaning at these frequency points, chaotic motion of the Duffing oscillator changes to periodic motion. Apart from these four points, the MLE is positive which means the system is still at chaotic state. This result indicates that precise chaos control of the Duffing oscillator can be achieved through accurately varying the frequency of the parametric pump. In order to further understand why the system is at periodic state at these four points and the accuracy of the chaos reconfigurability, Melnikov method is employed. Taking $\omega_p = 1$ as an example, Eq. (7) is solved for t_0 ranging from 0 to 1×10^6, other parameters remain exactly same as in previous calculations. It is seen from Figures 3(a) and 3(b) that as $\omega_p = 1.0001\omega$ and $\omega_p = 0.9999\omega$, there are many points where $M(t_0) = 0$, which indicates that it is possible for the system to reach chaotic states. However, when $\omega_p = \omega$, it is shown in Figure 3(c) that $M(t_0)$ does not have 0 solution, which means that the system will not reach chaotic state, hence it has been completed suppressed. Here, the ratio of pump frequency change is defined as $r_\omega = (\omega_p - \omega)/\omega$. It is noted that Eq. (7) has two forms ($\pm$); only minus sign is used in the calculation, as the equation with plus sign gives

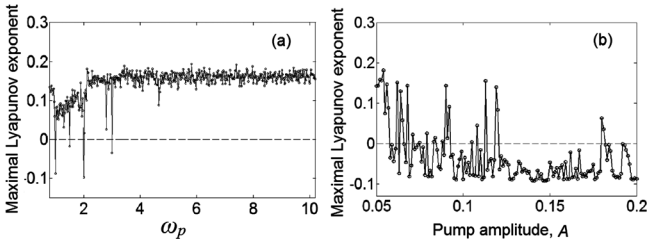

FIG. 2. Calculated MLEs of the Duffing system (negative spring constant) with a parametric pump with (a) varying frequency ω_p and (b) varying amplitude A.

impractical results. To demonstrate the sensitivity of the parametric chaos control, calculations are conducted for time section t_0 at the first point, where the $M(t_0)$ is zero versus the ratio pump frequency change. It is seen from Figure 3(d) that the relationship between logarithmic t_0 and logarithmic r_ω is almost linear. This indicates that as the pump frequency change gets smaller, the system takes longer time to return to chaotic state. When the pump frequency is exactly same as the frequency of the external exciting force, the chaos is completed suppressed. However, the case of ω_p being exactly same as ω is very difficult to achieve in practice, hence strictly speaking, the suppression cannot hold for long time in reality. The closer the ω_p to the ω, the longer time the suppression holds.

For further illustrating dynamic properties of the system when varying the parametric frequency, phase portraits for ω_p being 0.8 ω, ω, 1.5 ω, 2 ω are calculated, and results are shown in Figure 4. It is seen that the system is chaotic when $\omega_p = 0.8\ \omega$. When the ω_p increases to ω, 1.5 ω, 2 ω, phase portraits are calculated to be a single circle, and periodic solutions, respectively. The chaos control due to the amplitude of the parametric pump is also investigated. In this case, the frequency of the pump ω_p is fixed at ω, and the amplitude A varies from 0.05 to 0.2, while other parameters are same as in previous calculations. MLEs have been calculated, and results shown in Figure 2(b) indicates that less impact to the

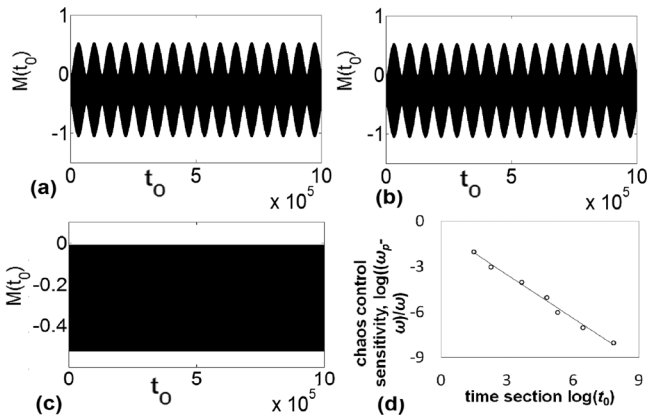

FIG. 3. Calculated $M(t_0)$ and chaos control sensitivity of the Duffing system (negative spring constant) with the parametric pump (A, ω_p). (a) Calculated $M(t_0)$ for $\omega_p = 1.0001\omega$. (b) Calculated $M(t_0)$ for $\omega_p = 0.9999\omega$. (c) Calculated $M(t_0)$ for $\omega_p = \omega$. (d) Chaos control sensitivity for ω_p near ω. Horizontal axis is the time section t_0 for the first $M(t_0) = 0$, and vertical axis is the difference between the pump frequency and the external driving frequency.

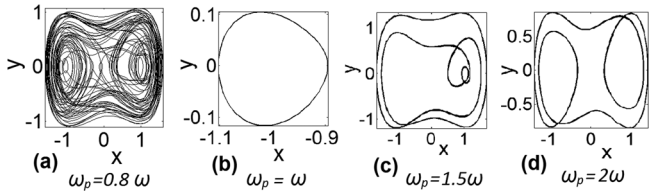

FIG. 4. Calculated phase portrait of the Duffing system (negative spring constant) with the parametric pump (A, ω_p).

Duffing oscillator when the parametric pump amplitude is small, and the impact becomes more significant as the amplitude increases. This is reasonable as the larger the amplitude of the parametric perturbation, the more significant influence it imposes to the Duffing system.

The positive linear spring constant system with parametric driven studied in this work was experimentally realized by Harrington and Roukes[7,19] as shown in Figure 1(b). It was constructed by a suspended doubly clamped beam supported by two parametric pump beams. The resonator was driven by a varied electrostatic force, and the parametric pumping force was generated by applying a periodical current to the two supporting beams, while the whole structure is exposed in a magnetic field. The varied pumping force stretches or compresses the doubly clamped resonating beam along its longitude, adjusting its linear spring constant. To study its nonlinear dynamics, a previous established one-dimensional elastic beam theory was used.[20,21] The following equation to describe the in-plane motion of the parametric pump driven doubly clamped resonator is as follows:

$$\ddot{z}(t) + (\omega_0^2 + k_p' \cos(w_p \omega_0 t)) z(t) + \delta \dot{z}(t) + \alpha z^3(t) = 2F_0 \cos(w_d \omega_0 t + \phi), \tag{8}$$

where $\delta = -f_1/(\rho S)$, $\alpha = 8E\pi^4/(9\rho L^4)$, $k_p' = k_p 4\pi^2/(3L)$, $F_0 = \sqrt{2/3} f_0/(\rho S)$, $\omega_0 = \sqrt{16\pi^4 EI/(3\rho S L^4)}$, $\omega_p = w_p \omega_0$, and $\omega_d = w_d \omega_0$. S and L are the cross-sectional area and length of the doubly clamped beam. E is the Young's modulus, and $I = wd^3/12$ is the moment of inertia of the beam's cross-section area. w and d are width and thickness, respectively. ρ is the mass density, ω_p is the pump frequency, and k_p is the pump amplitude which can be changed via modulating magnetic field B or the current applied to the pump beams. $f_0 = \pi\varepsilon_0 V_{dc} V_{ac}/(h(\ln(4h/d)^2))$ and $f_1 = -\pi P T_k/4 v_T$,[22] where the electrical potential is $V = V_{dc} + V_{ac}\cos(\omega_d t + \phi)$, in which V_{dc} and V_{ac} are dc and ac components, and ω_d as the drive frequency. h is the gap between the beam and the electrode. In this work, the gap is assumed to be constant as the vibration of resonator is very small. P and T_k are the air pressure and temperature, respectively, $v_T = \sqrt{k_B T_k/m}$ is the air molecule velocity at T_k. k_B is the Boltzmann constant. In order to arrive at Eq. (8), we have employed Galerkin's method[23] which assumes that the displacement in the z direction is $z(t) \times \varphi(x)$, $z(t)$ and $\varphi(x)$ are the time-dependent amplitude and eigenmode deflection, respectively. $\varphi(x) = (2/3)^{1/2}[1 - \cos(2\pi x/L)]$ is assumed, and it satisfies the boundary conditions $\varphi(0) = \varphi(L) = \varphi''(0) = \varphi''(L) = 0$.[20] Re-writing Eq. (8) into a two-degree-of-freedom model

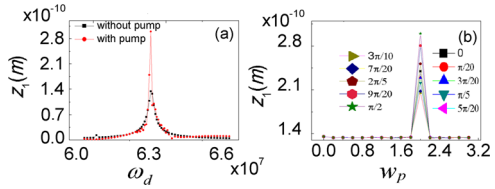

FIG. 5. Calculated parametric pumping effect to a Duffing system (positive spring constant) in periodic region. The results are consistent with experimental results in Ref. 16. (a) Displacement vs. parametric frequency. (b) Displacement vs. parametric amplitude.

$$\begin{aligned}\dot{z}_1 &= z_2\\ \dot{z}_2 &= -(\omega_0^2 + k_p' \cos(w_p\omega_0 t))z(t) - \delta\dot{z}(t)\\ &\quad - \alpha z^3(t) + 2F_0 \cos(w_d\omega_0 t + \phi).\end{aligned} \tag{9}$$

Based on the Eq. (9), first, we studied the parametric amplification by setting a low voltage V in which the resonator is vibrating in its linear regime, i.e., $V_{dc} = 100\,\text{mV}$ and $V_{ac} = 10\,\text{mV}$. We set the pump frequency and amplitude as $w_p = 2$, $\phi = \pi/2$ and $k_p' = 0.005\omega_0^2$. Other parameters are taken as $d = 10\,\text{nm}$, $w = 30\,\text{nm}$, $L = 3\ \mu\text{m}$, $\rho = 2332\,\text{kg/m}^3$, $E = 169\,\text{GPa}$, $T_k = 300\,\text{K}$, $P = 0.05\,\text{atm}$, $h = 1\ \mu\text{m}$, and $m = 5.6 \times 10^{-26}\,\text{kg}$.[22] From the calculated results in linear region (Figure 5(a)), we can see the amplitude has increased to 2.88×10^{-10} m in the driving frequency sweep ($0.95 < w_d < 1.052$), Furthermore, we investigated the amplitude increase under different phase ϕ and w_p, which are varied in [0, π/2] and [0, 2], respectively. Keeping other parameters unchanged, it is seen from Figure 5(b) that the peak of the increase occurs when $\phi = \pi/2$ and $w_p = 2$, which are consistent with the trend of parametric amplification both in theoretically and experimentally.[21,24] As the parameters used in this work are different, quantitative comparison was not made.

Furthermore, the device will be vibrating in nonlinear regime, specifically, the vibration of the resonator will be in transient chaotic state if the driving force increases to such an extent. For investigating the chaos controllability, in the following simulation, we increased the voltage to $V_{dc} = 20\,\text{V}$ and $V_{ac} = 12\,\text{V}$, and keep the rest of parameters unchanged but with $k_p = 0$ (without pump). It is found from the results

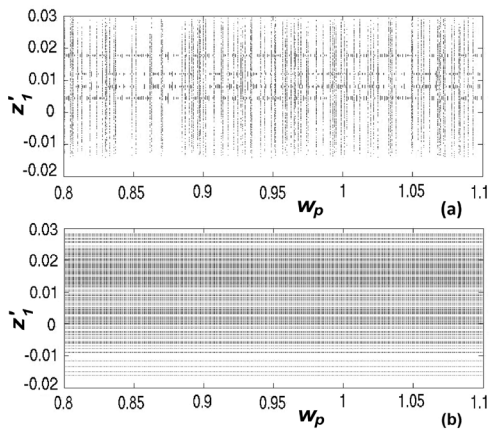

FIG. 6. Bifurcation diagram of displacement of the Duffing oscillator with positive spring constant when varying w_p in [0.8, 1.1]. (a), $k_p = 0.005w_0$, the time interval T is [0, 15 000]. (b), $k_p = 0$ with calculated time interval in the same range of (a).

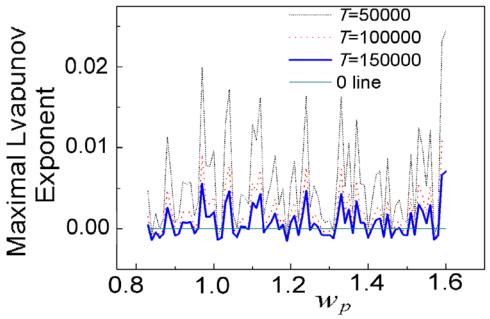

FIG. 7. MLE of the Duffing oscillator (positive spring constant) with w_p varying in [0.8, 1.6].

that the system is in the transient chaos before $T = 15\,000$ (T is a nondimensionalized time series, $T = \omega_0 t$), and then the chaotic state is transformed into periodic state when $T = 1\,500\,000$. It should be noted that we have employed the relation $z' = z/h$. When the parametric pump is turned on, the transient chaos disappears quicker compared with the system without the pump, especially on certain w_p and k_p. The bifurcation diagram of Eq. (9) when w_p is varying from 0.8 to 1.1 in time interval [0, 15 000] was calculated and shown in Figure 6. From Figure 6(a), it is seen there are many periodic states on certain pump frequencies. In contrast, as shown in Figure 6(b), the system is still chaotic without the parametric pump. Furthermore, the MLE as w_p varying from 0.8 to 1.6 was calculated. It is shown in Figure 7 that the MLE is becoming negative more and more as time increases, which means the transient chaos in the parametric pumping system will enter periodic state eventually but with less time. Besides, we explored the impact of k_p' when $w_p = 2$ is fixed. It is interesting to find from the phase portraits shown in Figure 8 that the k_p' has the effect to modulate the phase shape. With the increasing k_p', the number of intersections in the periodic trajectory increases, leading to increased number of periodic states.

To conclude, Duffing resonators with negative and positive spring constants driven by parametric pump were investigated to unveil the controllability of chaotic vibrations. Calculations were conducted to the two types of dynamic systems using established methods such as Melnikov's method, MLE, and Galerkin's method. All calculations used parameters from previous experiments except for varying driving conditions. For the negative spring constant system, a precise reconfigurability ($\pm 0.0001\omega$) has been demonstrated at the frequency point $\omega_p = \omega$. Calculation also shows that this reconfigurability can be further increased by extending t_0. Nevertheless, the time period during which the chaos being suppressed can be very long if the mismatch is sufficient small. The impact due to the amplitude of the

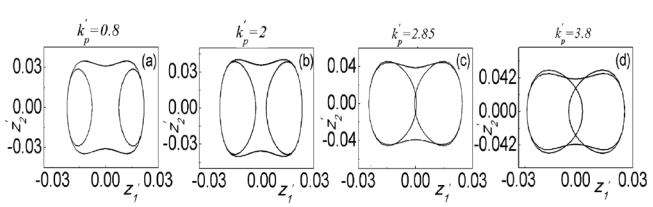

FIG. 8. Calculated phase portraits of Duffing oscillator (positive spring constant) when $w_p = 2$.

parametric pump has also been investigated. It is shown that as the amplitude increases, the impact becomes greater. For the positive spring constant Duffing system, transient chaos has been demonstrated, which can be controlled using the parametric pump. Varying parametric pump frequency and amplitude, it was found that the transient chaos entre the periodic state with less time than the system without parametric driving. This work theoretically validated dynamic behaviours of two typical systems, stable (positive spring constant) and unstable (negative spring constant). Results of this work will serve a future reference for design of the parametric driven Duffing oscillators.

The authors thank College of Engineering, Swansea University, the U.K. Leverhumle Trust, and Chinese Scholarship Council for support.

[1]E. Babourina-Brooks, A. Doherty, and G. J. Milburn, New J. Phys. **10**, 105020 (2008).
[2]R. Lifshitz and M. C. Cross, "Nonlinear dynamics of nanomechanical and micromechanical resonators," in *Reviews of Nonlinear Dynamics and Complexity*, edited by H. G. Schuster (WILEY-VCH Verlag GmbH & Co. KGaA, Weinheim, 2008), Vol. 1, Chap. 1.
[3]H. B. Peng, C. W. Chang, S. Aloni, T. D. Yuzvinsky, and A. Zettl, Phys. Rev. Lett. **97**, 087203 (2006).
[4]L. Jin, X. Wang, and L. Li, J. Appl. Phys. **113**, 093506 (2013).
[5]F. Cottone, H. Vocca, and L. Gammaitoni, Phys. Rev. Lett. **102**, 080601 (2009).
[6]F. C. Moon and P. J. Holmes, J. Sound Vib. **65**, 275 (1979).
[7]R. B. Karabalin, X. L. Feng, and M. L. Roukes, Nano Lett. **9**, 3116 (2009).
[8]R. B. Karabalin, S. C. Masmanidis, and M. L. Roukes, Appl. Phys. Lett. **97**, 183101 (2010).
[9]J. F. Rhoads, S. W. Shaw, K. L. Turner, J. Moehlis, B. E. DeMartini, and W. Zhang, J. Sound Vib. **296**, 797 (2006).
[10]B. E. DeMartini, J. F. Rhoads, K. L. Turner, S. W. Shaw, and J. Moehlis, J. Microelectromech. Syst. **16**, 310 (2007).
[11]B. E. DeMartini, H. E. Butterfield, J. Moehlis, and K. L. Turner, J. Microelectromech. Syst. **16**, 1314 (2007).
[12]C. B. Burgner, W. S. Snyders, and K. L. Turner, in *the 16th International Solid-State Sensors, Actuators and Microsystems Conference* (IEEE, 2011), p. 1990.
[13]C. Guo and G. K. Fedder, in *the 16th International Solid-State Sensors, Actuators and Microsystems Conference* (IEEE, 2013), p. 1703.
[14]C. Guo and G. K. Fedder, Appl. Phys. Lett. **103**, 183512 (2013).
[15]A. M. Elshurafa, K. Khirallah, H. H. Tawfik, A. Emira, A. K. S. A. Aziz, and S. M. Sedky, J. Microelectromech. Syst. **20**, 943 (2011).
[16]J. Guchenheimer and P. Holmes, *Nonlinear Oscillations, Dynamical Systems, and Bifurcations of Vector Fields* (Springer-Verlag, New York, 1983), p. 90.
[17]A. H. Nayfeh, *Introduction to Perturbation Techniques* (Wiley, New York, 1981).
[18]H. S. Haghighi and A. H. D. Markazi, Commun. Nonlinear Sci. Numer. Simul. **15**, 3091 (2010).
[19]D. A. Harrington, Ph.D. thesis, California Institute of Technology, 2002.
[20]M. D. Dai, C.-W. Kim, and K. Eom, Nanotechnology **22**, 265502 (2011).
[21]X. L. Feng, R. R. He, P. D. Yang, and M. L. Roukes, Nano Lett. **7**, 1953 (2007).
[22]Q. Chen, L. Huang, Y.-C. Lai, C. Grebogi, and D. Dietz, Nano Lett. **10**, 406 (2010).
[23]L. Meirovitch, *Analytical Methods in Vibrations* (Macmillan, New York, 1967).
[24]D. Rugar and P. Grütter, Phys. Rev. Lett. **67**, 699 (1991).